CNN-Based estimation of lower extremity kinematics during robot-based neurorehabilitation

Bachelor's Thesis in Biomedical Engineering
an der TUM School of Engineering and Design

Author:	Luis Vidal Solano
Supervisor:	Prof. Dr.-Ing. Sami Haddadin
Chair:	Chair of Robotics Science and Systems Intelligence
Advisor:	Kim Kristin Peper, M.Sc.
Submission Date:	20.09.2022 in München

I confirm that this bachelor's thesis is my own work and I have documented all sources and material used.

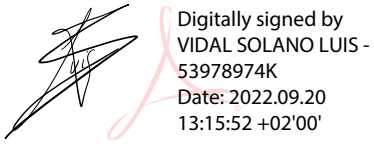

München, September 20, 2022 Luis Vidal Solano

Abstract

Understanding the kinematics of the lower extremity movement allows us to quantitatively assess performance changes, therefore being essential for proper diagnosis and rehabilitation treatments. However, the gold standard procedures for human motion capturing cannot be applied inside an Intensive Care Unit (ICU) scenario.

This work aims to validate a data-driven model for sagittal plane lower extremity angle measurement from accelerometer data, based on a deep learning approach. A convolutional neural network (CNN) was trained with ten and tested on two subjects, enabling the monitoring of the hip, knee, and ankle joint angles during therapy. The application was tested on the VEMOTION, an assist-as-needed robotic rehabilitation device. An optical motion capture system measured the reference joint angles.

The CNN model predictions deviated from the reference angles with a root mean squared error (RMSE) on the range of motion of less than 3.03º, 4.60º, 9.99º, and 4.49º for the hip, knee, ankle dorsiflexion, and ankle plantar flexion respectively.

This system has proven to be an easy and non-invasive way of estimating the behavior of the lower limb joint angles during VEMOTION rehabilitation.

Contents

Acknowledgments

I would like to express my gratitude to my supervisor, Kim Peper, who guided me throughout this project. I would also like to thank my friends and family who supported me on this journey.

1 Introduction

Over the last years, the cerebrovascular accident (stroke) incidence in most countries has more than doubled [19]. Over half of all stroke survivors have continuing problems with mobility [38]. However, movement rehabilitation requires a sustained and coordinated effort from a large team. As a result, the interest in rehabilitation robotics is increasing steadily [23].

One of the latest rehabilitation devices for very early mobilization is the VEMOTION system (Reactive Robotics GmbH, Munich, Germany). This device, among other things, solves the large-scale implementation of very early mobilization in critical care and allows only one person to perform early mobilization therapy even with severely affected patients, as they stay in the same bed [33].

To be able to do individual therapy for each patient, with devices like the VEMOTION, understanding the kinematics of the lower extremity movement is essential for proper diagnosis and rehabilitation treatments [2]. Also, the integration of clinical assessment with kinematic evaluation appears to be useful for quantitatively assessing performance changes [5].

Movement restrictions could be recognized early by assessing the kinematics during the early stages of rehabilitation. Especially stroke can lead to spasticity and restricted ankle range of motion (ROM), which may be severely disabling. In chronic stroke patients, limited ankle ROM is a common problem [1]. Nonetheless, during VEMOTION rehabilitation, only the hip angle is tracked.

In later stages of rehabilitation, optical motion capture systems are the gold standard for joint kinematics analysis [16] as well as for analyzing ROM of the ankle joint. However, it is not feasible to implement them in a clinical setup, especially in Intensive Care Units (ICUs). Therefore, other methods to estimate joint kinematics, like inertial sensors, must be employed [28].

Aware of all the problems already mentioned, this thesis will develop a CNN-based estimation of the lower extremity kinematics on the sagittal plane during treatment with the VEMOTION. The input will be accelerometer data provided by sensors attached to the device.

2 Theoretical background

This thesis is the result of the convergence of multiple disciplines, such as mechanics, biology, and deep learning. A few key fields will be addressed and explained in the following subsections to understand the work done thoroughly.

2.1 Lower limb rehabilitation devices

Robotics will play a significant role in rehabilitation therapy activities. The interest in this field has been growing exponentially over the last decade, mainly due to the success of the early systems and the increasing number of stroke patients and their rehabilitation costs. As a result, robot therapy systems have been developed worldwide to train both the upper and lower extremities [7].

The main objective of rehabilitation exercises is to perform specific movements that produce motor plasticity in the patient, improving motor recovery and minimizing functional deficits. Movement rehabilitation is limb dependent. Hence, the affected limb has to be exercised [30].

One-third of surviving patients from stroke do not regain independent walking ability, and those ambulatory walk asymmetrically [25]. Rehabilitation therapies are essential to recovery; therefore, considerable research is ongoing.

The traditional rehabilitation process is very labor intensive, especially for gait rehabilitation, and often involves more than three therapists. This fact imposes an enormous economic burden on any country's health care system, thus limiting its clinical acceptance [12].

Robotic systems allow precise measurement of movement kinematics and dynamics, which should be used for assessing patient recovery ability and progress.

Rehabilitation robots can free doctors from heavy training tasks, analyze robot data during training, and assess patients' rehabilitation progress. Rehabilitating stroke victims or patients recovering from surgery can benefit from rehabilitation robots due to their accuracy and reliability [41].

However, there is a need to develop standard protocols and procedures to obtain reliable assessment data. Currently, clinical measures such as the Barthel index [34] usually quantify patient recovery of walking ability.

It is important to note that passive robotic rehabilitation devices, although less complex and cheaper, cannot supply energy to the affected limbs, which limits their effectiveness compared with active rehabilitation devices.

A variety of lower-limb rehabilitation robots have been developed in recent years to enhance the motor function of paralyzed limbs in stroke patients. There are two general categories of robots

for lower-limb rehabilitation: exoskeleton robots and end-effector robots [40]. For example, Lokomat [9], BLEEX [18], and LOPES [37] are typical exoskeleton robots, while Rutgers Ankle [15] and Haptic Walker [17] are end-effector robots.

In this thesis, the VEMOTION (Reactive Robotics) device was used. Therefore, the implementation is specific to this device, although it could be transferred to other rehabilitation strategies with similar movement patterns.

The VEMOTION (Fig. 2.1), by Reactive Robotics, consists of a patient mobilization robotic device that implements an assist-as-needed rehabilitation strategy. It adapts the amount of force applied depending on the patient participation. This device solves the large-scale implementation of Very Early Mobilization in critical care since it allows only one person to perform early mobilization therapy even with severely affected patients, as they stay in the same bed [33].

Figure 2.1: VEMOTION robotic system, Reactive Robotics [33].

The movement of the VEMOTION consists of a cyclic motion composed of a series of motorized joints and a passive joint. The footplate has both freedom of rotation with a revolute joint and freedom of translation with a sliding rail. During the rehabilitation, the patient can choose whether to move the sliding rail or not. Thus, causing that the treatment might not be as effective if not. This influences the joint kinematics of the ankle. Therefore, being of interest to estimate the joint angles during this movement.

2.2 Motion Capture Systems

Motion capture is the process of recording the movement of objects or people. It involves measuring the position as well as the orientation of the objects or people in physical space [27].

Motion capture systems are the gold standard for gait analysis. There are different methods of motion capture systems, mainly distinguishing between marker-based and marker-less tracking. Marker-based tracking uses four different approaches to determine the position of the markers, those being acoustic, magnetic, mechanic, and optical [27].

The most common systems used in the last decade for motion capturing were optical systems (such as VICON, PHASESPASE, or QUALISYS). The optical motion capture system utilizes data from image sensors to triangulate the 3D position of the body segments using several cameras. Body segments are identified in the image with reflective or infra-red markers attached to the body [16].

Their high sampling rate and the freedom of not having the restrains of cables or limited workspace allows the capture of fast movements. There are a few systems on the market [27].

The VICON System (VICON Motion Systems Ltd., Oxford, United Kingdom) works using passive infrared markers that get recorded by specialized cameras distributed in the room pointing at the set origin. The cameras make use of a technology that collects the reflected infrared lights' position on the markers' surface. From the images of every camera, a 2-D vector with the marker's position is calculated. Using Nexus, adding up the computed 2-D coordinates with the synchronized placement of the cameras, it is possible to create a 3-D vector. Through this process, the position of the markers in a dynamic motion can be determined with high precision. Another positive factor about Nexus is that it allows the data to be converted into various file formats [35].

This system allows the determination of biomechanical variables (angular velocity, linear acceleration, or orientation) by tracking the markers. Although the performer moves freely without any restrictions, as there are no cables connecting the body to the system, the system is restricted to be used inside a specific camera setup, which is expensive and complicated to install [16].

The spread of cheaper systems needs validation studies that compare the accuracy of new systems with scientific gold standard systems, representing an approach to which researchers can relate. Other critical technical aspects of adequacy in a specific application are capture volume, minimum detectable marker size, frequency, and resolution of the motion capture system. Sometimes in biomechanical studies, the selection of the motion analysis system is questioned when a system different from the gold standard Vicon system is used [26].

Recently, wearable sensors have gained attention as an unobtrusive method. Therefore, Convolutional Networks for signal processing problems have shown promising results in human motion estimation [14].

"Inertial sensors" refer to a family of sensors represented by linear acceleration sensors (accelerometers) and angular rate sensors (gyroscopes). Accelerometers and gyroscopes measure linear acceleration and angular velocity along and about a so-called "sensitive axis," respectively [28].

There are three main approaches to measuring human kinematics using inertial-based sensors.

1. Using IMUs placed on the distal and proximal segments and calculating their relative orientation.

2. Using kinematic constraints for model-based measurements.

3. Data-driven methods that employ supervised learning models.

2.2.1 IMUs

Inertial sensors, also known as inertial measurement units (IMUs), quantify acceleration, angular rate and the magnetic field vector in their own three-dimensional local coordinate system [32].

The orientation-based method has traditionally been used to compute human kinematics but has some limitations, being the sensor-to-segment alignment the main one [13].

As the anatomical orientation of the bone differs from the local reference frame of the IMUs, it requires a calibration step to calculate the relative orientation of the IMU and the anatomical reference frame. However, the precision of the calibration also relies on performing predefined movements correctly, which may not be reliable, especially in injured populations [32] .

In any case, this thesis aims to estimate the joint kinematics with sensors exclusively attached to the device, so the IMU approach would not be suitable.

2.2.2 Model-based

Kinematic or musculoskeletal model-based approaches take into account the kinematic constraints of the human body to deal with the limitations of sensors, such as drift and sensor-to-segment alignment [22].

However, implementing this would require a large number of sensors and a complex kinematic reconstruction to get results with the precision required [8].

2.2.3 Data driven

The third lower extremity joint angle monitoring method is a data-driven approach that relies on machine learning algorithms [10] [39]. This method feeds the raw signal into a machine learning model. This model takes care of the sensor-to-segment calibration and calculates the joint angles. The main limitation of the data-driven method is the dependency on the supplied dataset and generalizability to other subjects or populations.

Gholami et al. [13] used a shoe-mounted accelerometer for sagittal plane lower extremity angle measurement during running based on a deep learning approach. They reported an average root mean squared value for hip, knee, and ankle angles greater than 0.97, while the RMSE and NRMSE were lower than 3.4° and 4.6 %, respectively. The study demonstrated the potential of kinematic parameter estimation during dynamic movement using data-driven methods.

2.3 Joint Kinematics

The study of human motion is a branch of biomechanics known as kinematics. A complete and accurate quantitative description of even the simplest movement requires large volumes of data and variables in the kinematic analysis. The complete kinematics of any body segment in a three-dimensional spatial system requires 15 data variables [2]. Nonetheless, this thesis aims to measure only the angles during the motion.

A kinematic model of the joint should be created when the motion of an anatomic joint, specifically a diarthrodial joint, is to be measured. The shape and contour of the contact surfaces, as well as restrictions imposed by the surrounding soft tissue are the main factors affecting joint function. All anatomic joints actually contain six degrees of freedom (DOF), meaning that in order to determine the relative locations of the attached body segments, six independent characteristics must be measured and reported. However, depending on the goals of the research and the required level of accuracy, simplified models are typically employed [2].

This thesis focuses on the sagittal plane, as there is little to no movement on the other axis during VEMOTION rehabilitation. The results will look similar to the ones in figure 2.2, which shows the sagittal plane joint angles while walking, but applied to the VEMOTION rehabilitation device.

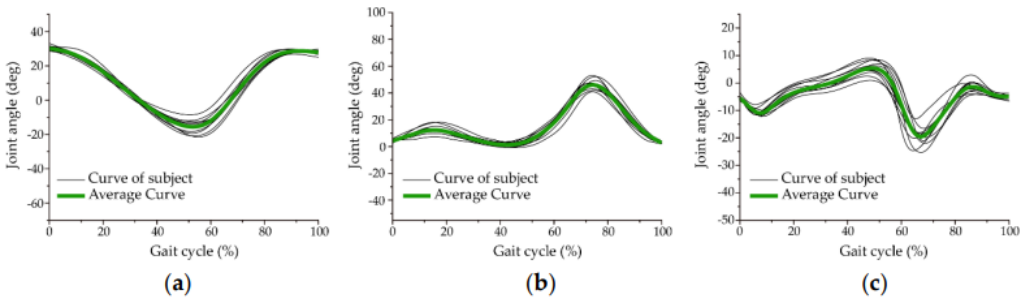

Figure 2.2: Sagittal plane joint angles while walking. Hip flexion/extension (a), knee flexion/extension (b), ankle dorsi/plantar flexion (c)[11] .

The angles between two or more body segments are called joint angles. Figure 2.3 shows the different joint movements of the lower limb in the sagittal plane. The angle formed by the projected transverse thigh and transverse pelvic axes is known as hip extension and flexion. When the knee is posterior to the body, the flexion value is positive. The angle formed by the transverse axes of the transverse thigh and the transverse shank is the knee extension and flexion. The knee is flexed in the direction that is positive. The angle between the sagittal foot axis and the transverse shank axis in platingrad position is known as the ankle dorsi and plantar flexion. Plantar is the negative direction, and dorsi is the positive direction [31].

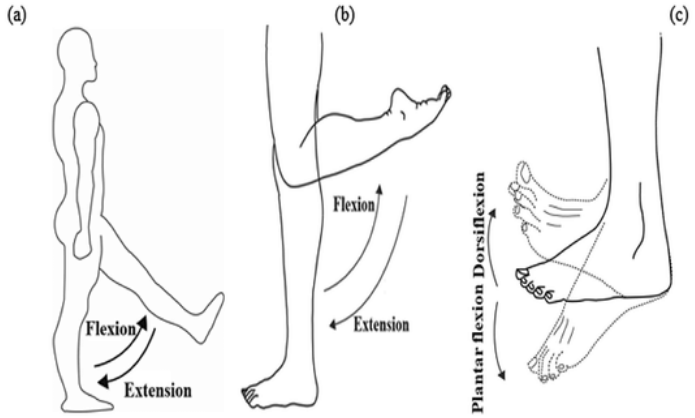

Figure 2.3: Hip flexion/extension (a), knee flexion/extension (b), ankle dorsi/plantar flexion (c) [20].

Impaired function of the ankle joint can decrease mobility in older adults [36]. During a rehabilitation procedure, especially during early mobilization, it is vital to be conscious of this dorsiflexion movement. Otherwise, we can find changes in function such as increased passive resistance of the elastic tissue in opposing muscles, tendons, and articular structures, weakened agonist muscles, and impaired proprioceptive control [36]. As demonstrated by Alamer et al.[1], ankle joint mobilization with movement therapy could improve ankle ROM, balance, and spatial gait parameters in chronic stroke survivors.

2.4 Deeep learning

Deep learning allows computational models composed of multiple processing layers to learn data representations with multiple levels of abstraction. By employing the backpropagation technique to suggest how a machine should modify its internal parameters, it can find complex structures in huge data sets. This is used to compute the representation in each layer from the representation in the previous layer [24].

A collection of techniques called representation learning enables a computer to be fed with unstructured data and automatically find the representations required for detection or classification. Deep learning techniques are representation-learning techniques that use multiple levels of representation. They are created by combining simple but non-linear modules that convert the representation at one level (beginning with the raw input) into a representation at a higher, slightly more abstract level. Very complex functions can be learned if enough of these

transformations are combined [24].

Convolutional Neural Networks (CNNs) have emerged as the *de facto* standard for many Computer Vision and Machine Learning operations over the past decade. CNNs are feed-forward Artificial Neural Networks (ANNs) with alternating convolutional and subsampling layers [21].

CNNs are designed to process data that come in the form of multiple arrays [24]. Deep CNNs with many hidden layers and millions of parameters can learn complex objects and patterns and be trained on a massive visual database with ground-truth labels [21].

Recently, 1D CNNs(fig. 2.4) attained state-of-the-art performance levels in several applications, including the classification and early diagnosis of personalized biomedical data, the monitoring of structural health, the identification and detection of anomalies in power electronics, and the detection of electrical motor faults. Another key benefit is that a real-time and affordable hardware implementation is possible because of the simple and compact configuration of 1D CNNs, which only perform 1D convolutions (scalar multiplications and additions)[21].

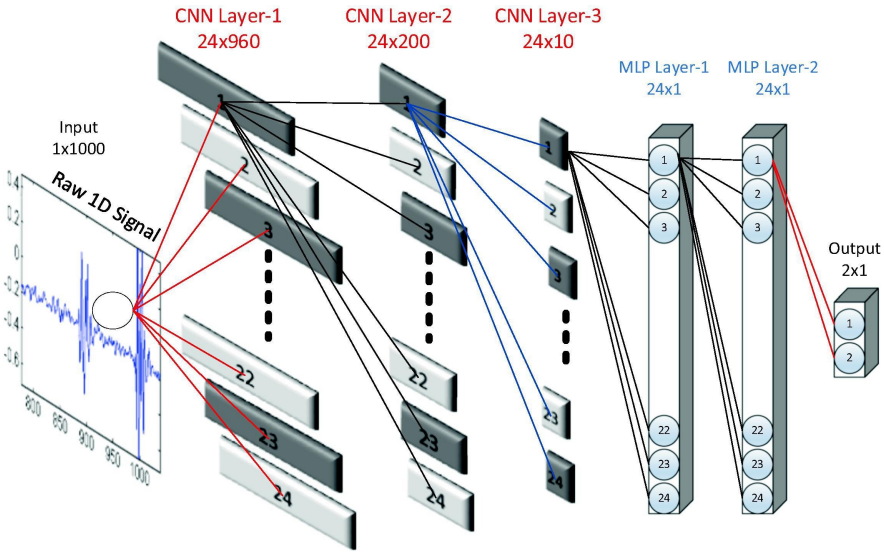

Figure 2.4: A sample 1D CNN configuration with 3 CNN and 2 Multilayer Perceptron layers[21].

3 Methods

For this study, 12 subjects (Tab. 3.1) (7 male ,5 female; age 30.00 ± 3.54 years, height $172,92 \pm 11,06$ cm, and weight $74,25 \pm 14,64$ kg) were tested in the VEMOTION device.

Subject number	Gender	Height (cm)	Age (years)	Weight (kg)
1	Male	176	28	96
2	Male	170	31	70
3	Male	173	34	70
4	Male	183	29	81
5	Male	186	28	92
6	Male	185	38	90
7	Female	155	30	55
8	Female	163	32	82
9	Female	169	27	60
10	Male	189	25	80
11	Female	160	27	55
12	Female	166	31	60

Table 3.1: Gender, height, age and weight of the subjects tested.

Every subject performed two trials of 90 seconds with a speed of 30 steps per minute and a verticalization angle of the bed of 50 degrees. During the first half of the trial, the subject was asked to actively lift the sliding rail of the VEMOTION device, making the ankle joint angle larger during the motion. On the other hand, for the second half of the trial, the subject did not perform any movement on the sliding rail, only tilting the footplate on the rotation axis.

In figure 3.1 the position of the joints at the top part of the motion can be appreciated in both cases.

Figure 3.1: Overlay picture of Vicon Nexus and Video during maximum hip angle and two different options of moving the ankle joint: (a) only rotation and (b) actively lifting the sliding rail

The reasoning behind these instructions is that the network needed to be trained with both possible case scenarios, with an equal dataset for each, avoiding overfitting.

The training of the network was made with the first ten subjects. This network was applied to the unseen data from the remaining two subjects.

3.1 Experimental setup and data collection

To develop the custom CNN network, ground truth data was captured with the Vicon motion capture system (Vicon Motion Systems Ltd, Oxford, UK), and the final input for the network was measured with accelerometer sensors (Mini Wave Infinity, Cometa Systems, Italy). They will be explained in detail in the following subsections. In figure 3.2 a half of the setup with the VEMOTION system and cameras can be seen.

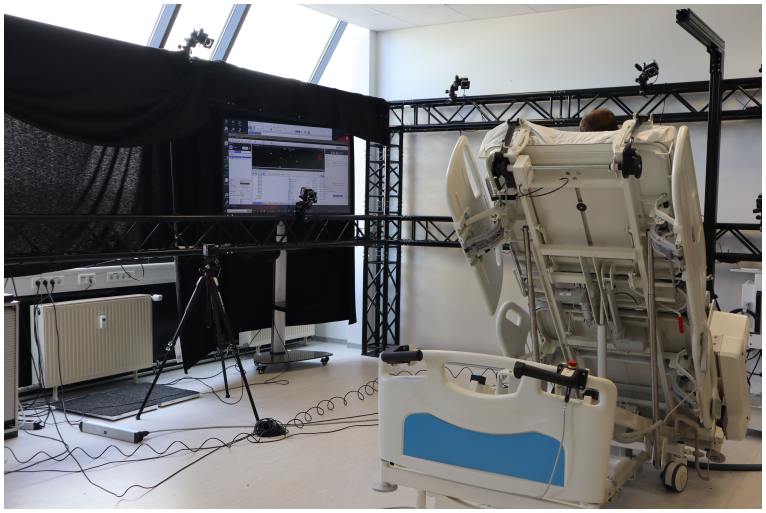

Figure 3.2: Experimental setup of the subject testing in the laboratory.

3.1.1 Vicon system

The kinematic data of the lower limbs were captured with the Vicon motion system (Nexus 2.12.1) with 17 cameras (16x Vicon Vero 2.2, 1x Vicon Vue) at 200Hz.

Regarding the placement of the markers, the Plug-in Gait lower body (Fig. 3.3) model provided by Vicon Nexus was used. All Plug-in Gait marker sets are designed for the Newington-Helen Hayes model [3] on which Plug-in Gait is based. The marker set for Plug-in Gait lower body modeling includes markers for the pelvis and the lower limbs. Specifically, the two posterior superior iliac spine (PSIS) markers for the pelvis variation were employed.

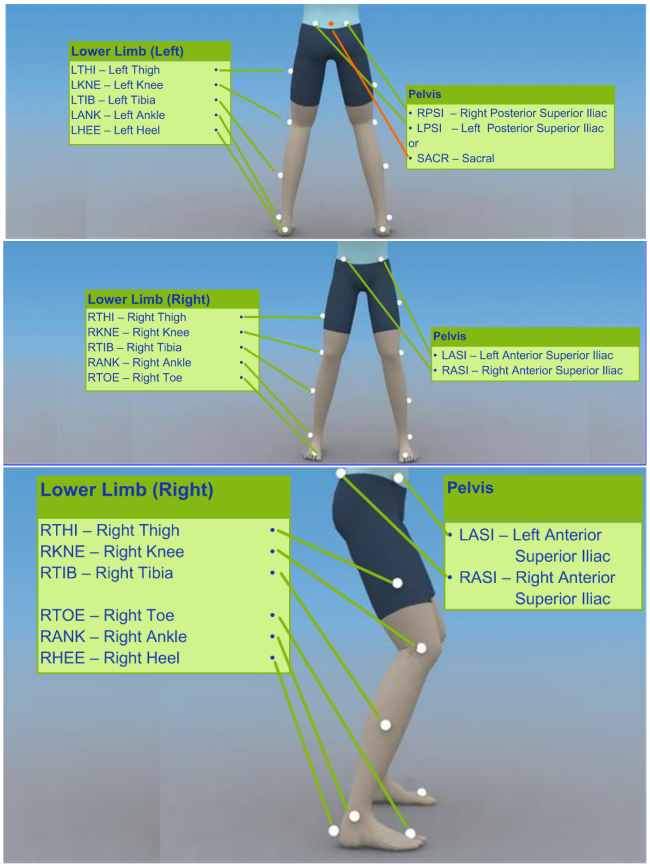

Figure 3.3: Front, back, and right side view of the marker placement for Plug-in Gait lower body model [35]

However, due to the subject's position on the bed, the RPSI, LPSI, LHEE, and RHEE markers were impossible to track. Therefore, reconstruction after the measurements was necessary. First, new markers were added to the subject in the following positions:

- Iliac crest (RPEL and LPEL).
- Medial part of the knee (RKNEMedial and LKNEMedial)
- Medial malleolus (RANKMedial and LANKMedial)
- Hallux (RTOEMedial and LTOEMedial)

The exact location of the new added markers can be appreciated in figures 3.4 and 3.5.

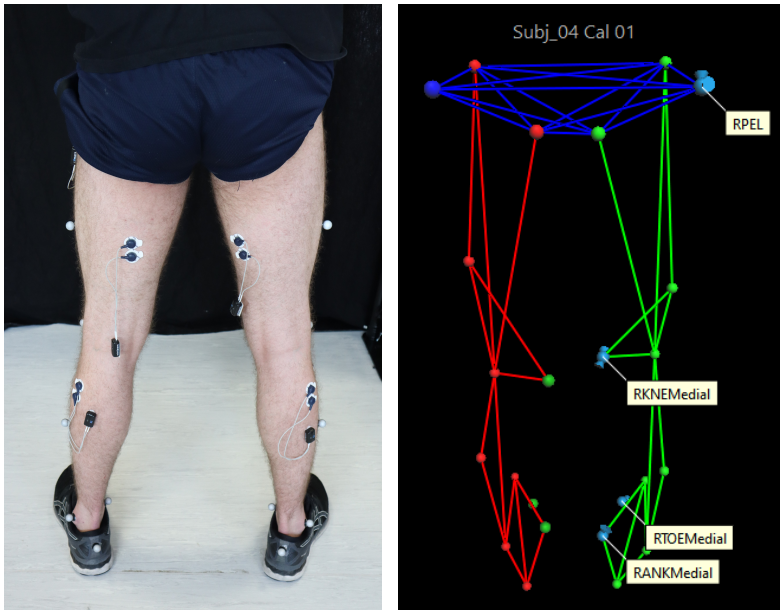

Figure 3.4: Back view of marker placement for the experiment, with the extra markers added

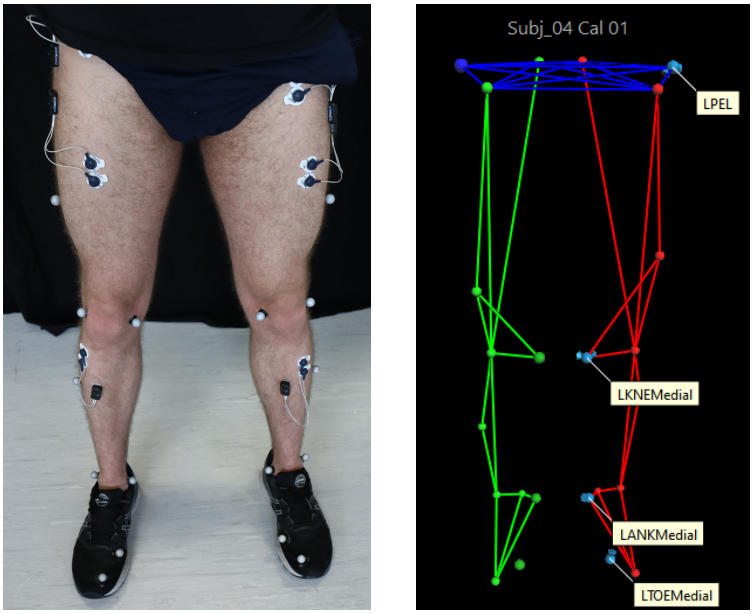

Figure 3.5: Front view of marker placement for the experiment, with the extra markers added

Afterwards, a calibration capture was made with the subject standing, using all the markers shown on figure 3.3 and the new ones showed in figures 3.4 and 3.5 , as can be seen in 3.6.

Then, the RPSI, LPSI, LHEE, and RHEE markers were removed, the subject was placed on the bed, and the movement measurements were taken, as seen in figure 3.7.

During the trials, there were some issues detecting the RANK and LANK markers. Consequently, the "Replace 4 Macro" (Nev Pires – Vicon Motion Systems, Inc.) script was used. This code recovers those markers on a rigid body segment that are missing for a few frames in the trial. However, if two or more markers on the rigid body segment are missing in the same frame/s, they will not be replaced.

On the other hand, the reconstruction process was made using the Replace Missing Maker script (Nev Pires – Vicon Motion Systems, Inc.). This script replaces a marker missing on a four-marker rigid body cluster during a dynamic trial but is present in a static trial. The previously made calibration was used as a static trial for the recreation of RPSI, LPSI, LHEE, and RHEE, using the markers that belong to the same rigid body. The results can be seen in figures 3.8 and 3.9

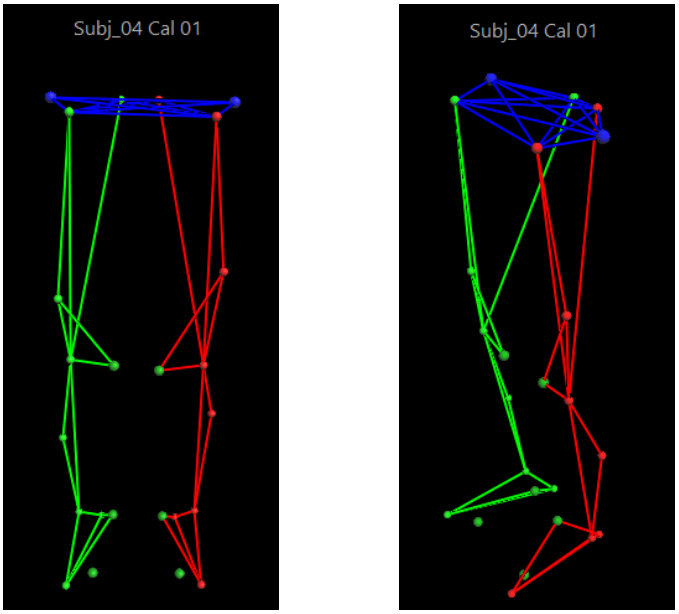

Figure 3.6: Screenshot of the Vicon Nexus Plug and Gait model template after calibration

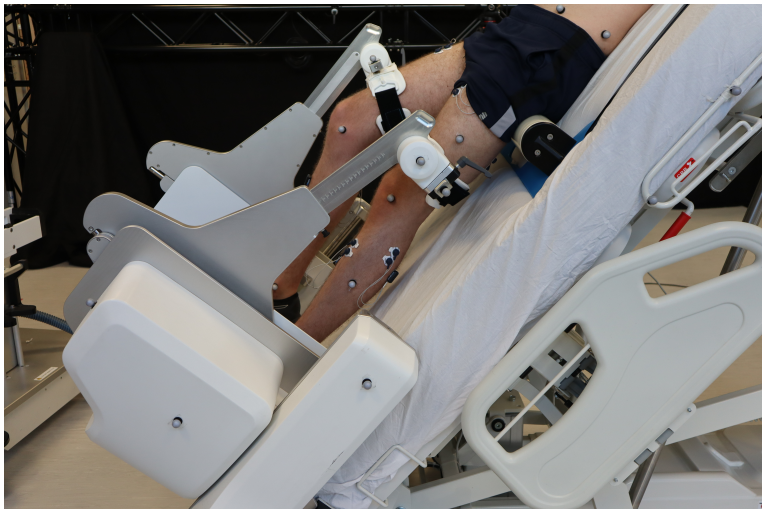

Figure 3.7: Photo of one subject during the study in the VEMOTION with attached sensors

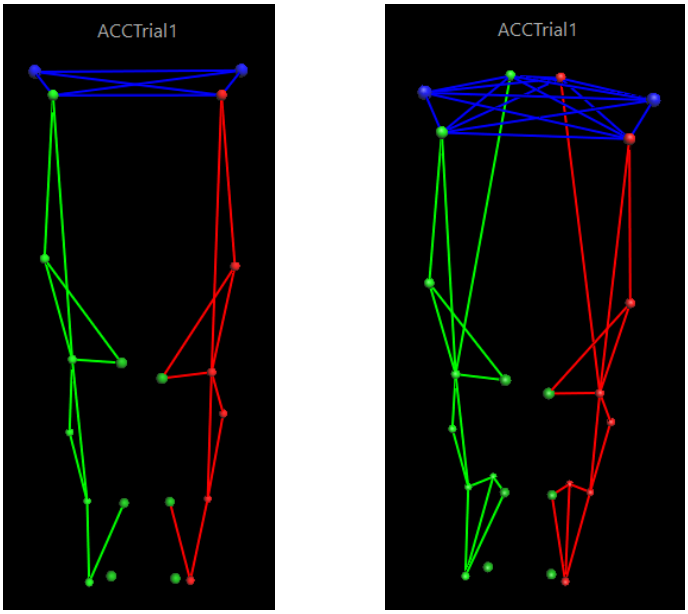

(a) (b)

Figure 3.8: Front view of the labeling template (a) before and (b) after the reconstruction

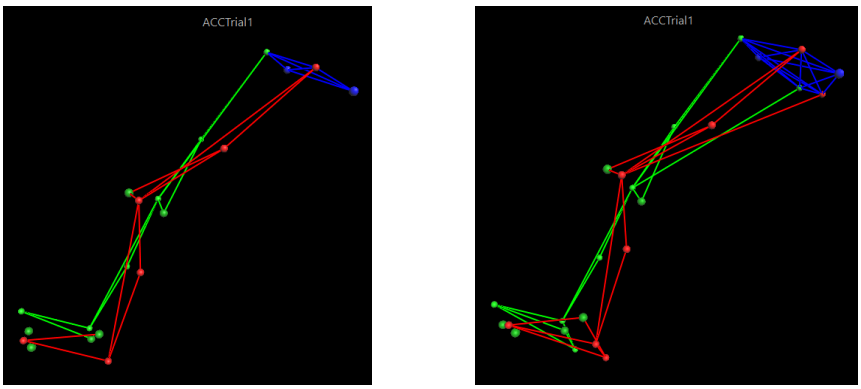

(a) (b)

Figure 3.9: Side view of the labeling template (a) before and (b) after the reconstruction

3.1.2 Accelerometer data

The accelerometer data was measured with the Mini Wave Infinity (Cometa Systems). This device is the state of the art of wireless data loggers on the market. Although it has been developed to measure EMG data, it also provides accelerometer data with a sampling rate of 2KHz.

As explained in the introduction, the footplate has both freedom of rotation with a revolute joint and freedom of translation with a sliding rail (fig. 3.10). During the rehabilitation, the patient can choose whether to move the sliding rail or not, which is why these two types of movements have to be distinguished.

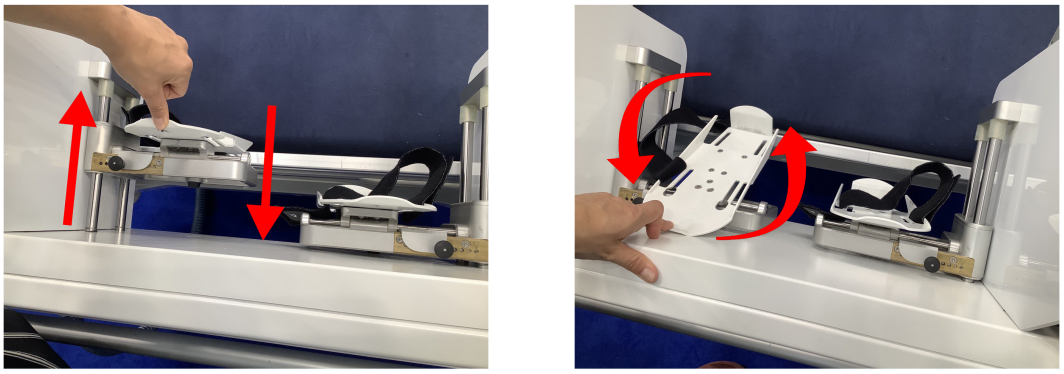

Figure 3.10: Translation with sliding rail (a), rotation with revolute joint (b)

One accelerometer sensor was placed on the sliding rail, capturing the translation movement, and the other was placed on the edge of the posterior part of the footplate, capturing the rotation movement, as demonstrated in figure 3.11. The exact layout was used on both legs. The output of the accelerometer sensor is divided into the three dimensional axes.

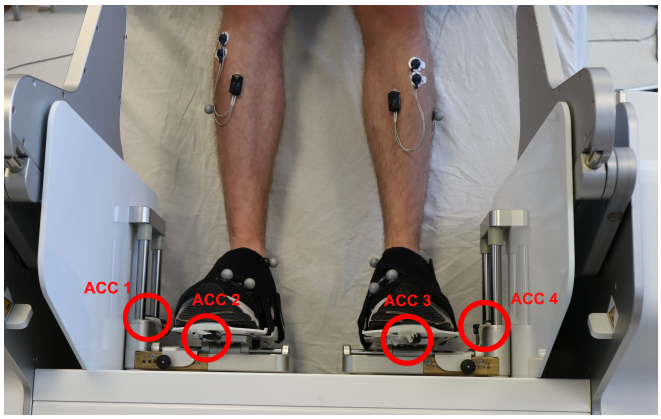

Figure 3.11: Placement of the accelerometer sensors

3.2 Data preprocessing

Before feeding the data into the CNN model, it first went through some preprocessing. Both signals were down-sampled to 100Hz. Afterward, a 20 Hz low-pass filter was used to reduce the noise, following the recommendation of previous studies [14].

The input for the knee and hip angles consisted of the data provided by the accelerometers placed on the sliding rail (numbers 1 and 4 on figure 3.11)

The values from the accelerometer's signal (fig. 3.12) placed on the sliding rail (Z axis) below the mean of the signal were replaced by the mean itself. This procedure removes noisy fluctuations and improves data clarity.

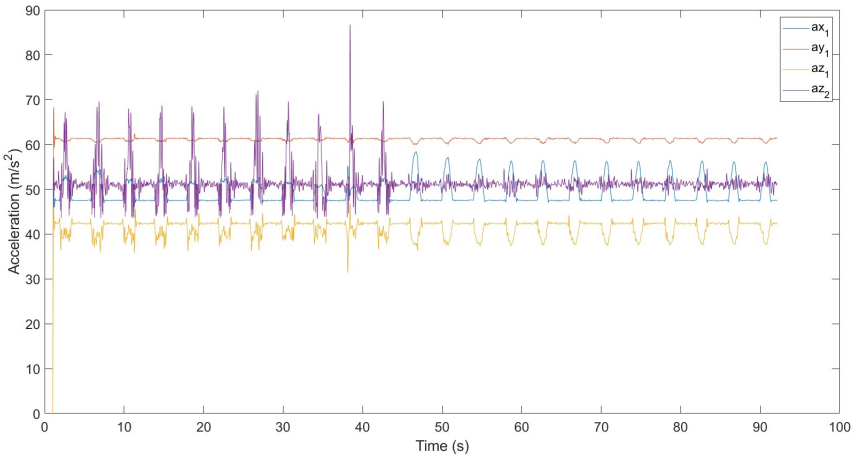

Figure 3.12: Sample of preprocessed accelerometer signal

Regarding the ground truth data (Vicon Nexus export), an offset of +90 degrees was applied to the ankle angle, changing the reference system. This was made because we required positive values for the network, as ReLU layers were used.

3.3 Deep Learning Model

Convolutional neural networks (CNNs) have been recently applied to different signal processing problems and have also shown promising results in human motion estimation using wearable sensors [14].

As explained in the theoretical background, Gholami et al. [13] used a shoe-mounted accelerometer for sagittal plane lower extremity angle measurement during running based on a deep learning approach. The present thesis made a similar approach using accelerometers placed on the VEMOTION device instead of the subject.

In this thesis, three different one-dimensional CNN (1D-CNN) were implemented in MATLAB and Deep Learning Toolbox, Release 2022a (The MathWorks, Inc., Natick, Massachusetts, United States)

Every CNN was designed for each of the predicted angles. The output consisted of the value

of the angle itself in a specific moment. On the other hand, the CNN was fed a 40x4 matrix with accelerometer data, using the sliding window principle, as follows:

$$\begin{bmatrix} a_{1x}(n-t) & ... & a_{1x}(n-1) & a_{1x}(n) & a_{1x}(n+1) & ... & a_{1x}(n+t) \\ a_{1y}(n-t) & ... & a_{1y}(n-1) & a_{1y}(n) & a_{1y}(n+1) & ... & a_{1y}(n+t) \\ a_{1z}(n-t) & ... & a_{1z}(n-1) & a_{1z}(n) & a_{1z}(n+1) & ... & a_{1z}(n+t) \\ a_{2z}(n-t) & ... & a_{2z}(n-2) & a_{2z}(n) & a_{2z}(n+2) & ... & a_{2z}(n+t) \end{bmatrix}$$

$$a_1 = Accelerometer\ 1\ (Footplate)$$

$$a_2 = Accelerometer\ 2\ (Sliding\ rail)$$

See figure 3.11 for detailed positioning on the device.

A time window was moved over the signal with a length of t=200 ms that covered equal samples of the past and the future time steps, thus making a window size of 400 ms that, after the downsampling to 100 Hz, corresponds to 40 elements.

Although the input for the ankle joint estimation did not include the z-axis component of the accelerometer placed on the footplate, since it did not supply any meaningful information for this joint, the sliding window principle applied was the same.

The training was divided into three different networks for each joint (hip, knee, and ankle), as they required different input preprocessing for optimal results. However, they all had the same structure:

The 1D-CNN model had four convolutional (Conv) layers and a max-pooling layer. The number of features at the first and second two Conv layers was 50 and 100, respectively. The architecture and layer shapes are summarized in table 3.2. All the trainable layers were initialized with a Xavier normal initializer. The Conv and fully connected layers were activated with a rectified linear unit, while the output layer was activated with a linear function. The kernel size and stride values were selected as 3 and 1, respectively. The parameters were optimized by an Adam optimizer with a learning rate of 0.001. The batch size for training the model was selected to be 512, and the number of epochs was fixed to 60.

Table 3.2: Convolutional neural network layers

Index	Layer	Output Shape	Setting
0	Input	(40,4)	
1	1D-Conv	(38,50)	ReLU
2	1D-Conv	(36,50)	ReLU
3	MaxPool	(18,50)	
4	1D-Conv	(16,100)	ReLU
5	1D-Conv	(14,100)	ReLU
6	Flatten	1400	ReLU
7	Dense	100	ReLU
8	Dense	1	Linear

3.4 Data Analysis

This network predicts the hip, knee and ankle range of motion during the movement. For every subject, the minimum and maximum values of the angles vary, and this information is impossible to extract from the accelerometer data.

Therefore, the main objective of this thesis is to estimate the difference between the capability of a joint to go through its complete spectrum of movements, known as range of motion (ROM). However, the RMSE results are also interesting to observe.

Four different evaluation metrics were considered in this study:

1. Root mean squared error (RMSE)
2. Normalized root mean squared error (NRMSE).
3. Root mean squared error of the range of motion (ROM-RMSE)
4. Root mean squared values (R^2)

The first three evaluation metrics reflect the measurement error, while the fourth reflects the goodness of predicted values. To calculate the NRMSE, the RMSE was divided by the range of angles in the test dataset. Equations of RMSE and NRMSE are as follows:

$$RMSE = \sqrt{(\frac{1}{n})\sum_{i=1}^{n}(y_i - \hat{y}_i)^2}$$

$$NMRSE = \frac{(RMSE)}{y_{max} - y_{min}}$$

On the other hand, to calculate the ROM-RMSE, it was first necessary to get the values of the joint range of motion during every movement of the trial for both predicted and ground truth data.

Firstly, the peaks and local minima were found, as in the example in figure 3.13

Secondly, two markers were created before and after the peak or minimum, as seen in figure 3.14. The mean of the section between the marker that indicates the end of the movement and the following one was calculated.

Finally, the difference between the peak or minimum value and the resting position resulted in the value of the ROM.

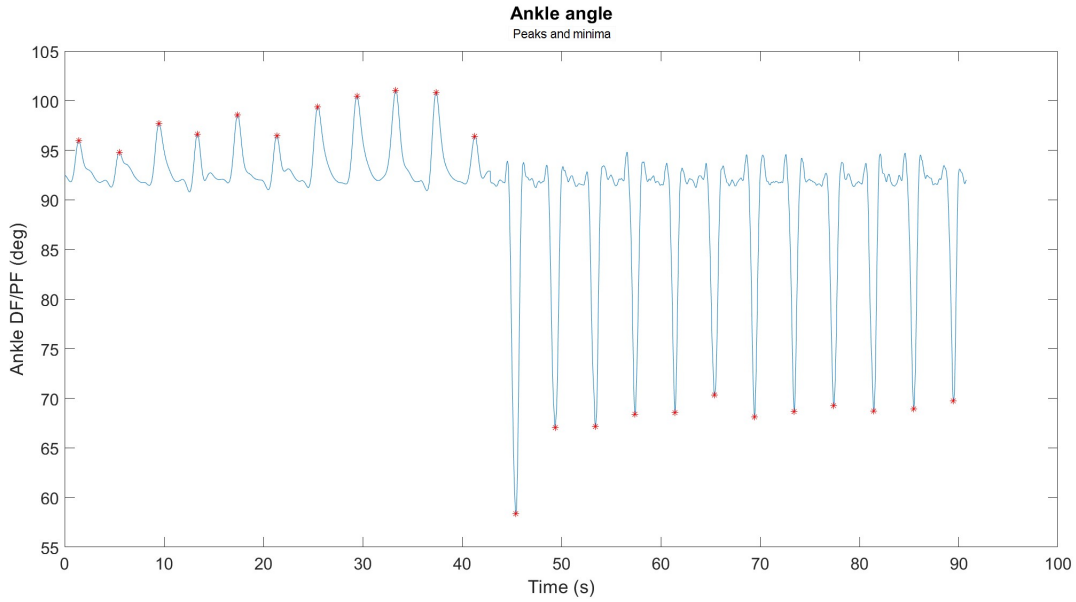

Figure 3.13: Peaks and local minima. Ankle angle prediction of subject 12, trial 1

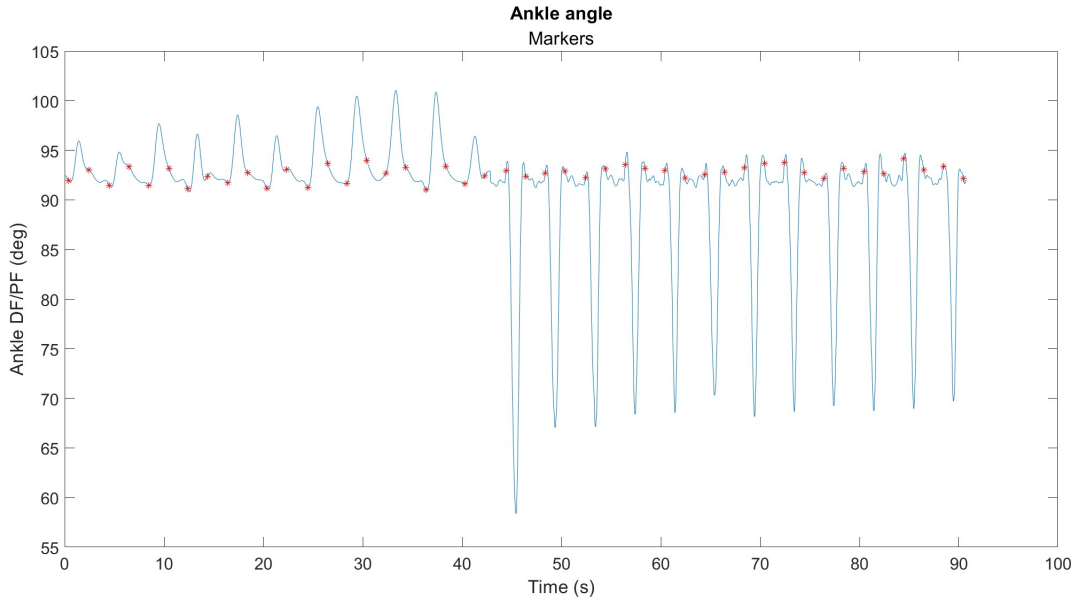

Figure 3.14: Markers of beginning and end of the movement. Ankle angle prediction of subject 12, trial 1

4 Results

In this chapter, the results of the three CNNs predictions will be presented. The results are divided into three sections for the three analyzed joints hip, knee, and ankle. In all three sections, the results of the training for subject one to ten and the results of the CNN estimation in subjects eleven and twelve are shown. To give a first overview, the results of the normalized RMSE (NRMSE) as % of the maximal ROM of all three joints of the subject eleven and twelve for trial one and two including the mean and standard deviation are displayed in figure 4.1.

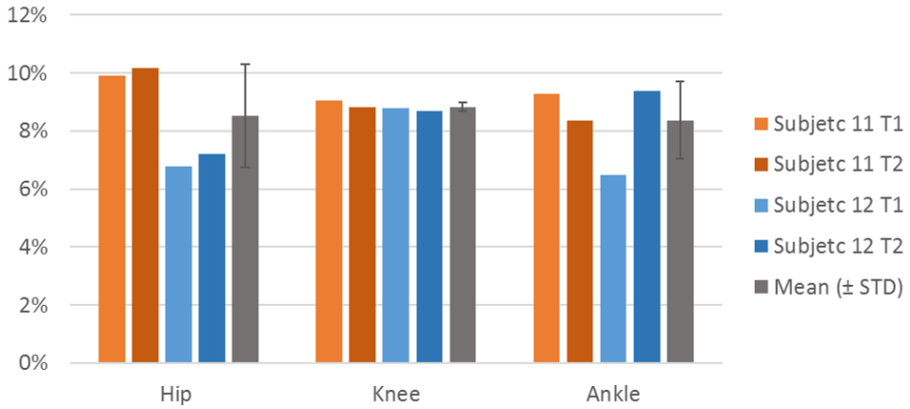

Figure 4.1: Normalized RMSE in % of the hip, knee and ankle joint for the test subjects eleven and twelve

4.1 Hip Joint

In table 4.1, the results of the hip angle predictions for the training data are displayed. The average root mean squared value (R^2) for ten participants was greater than 0.85, while the RMSE and NRMSE were lower than 4.275° and 13.47 %, respectively. Regarding the range of motion (ROM), the obtained value of the RMSE-ROM was 3.715°.

The outcome performance for the hip angle among subjects eleven and twelve, which are the test results, are displayed in table 4.2. In this case, the R^2 was 0,925, the RMSE and NRMSE 2.843° and 8.52% respectively, and the RMSE for the range of motion 3.025°.

Figure 4.2 displays the prediction and the ground truth for the hip angle, corresponding to subject eleven during the first trial.

Table 4.1: Training results of the hip joint with mean and standard deviation (STD)

Subject	Trial	RMSE (deg)	NRMSE (%)	R^2	ROM-RMSE (deg)
1	1	4.397	17.79	0.810	7.723
	2	5.199	18.79	0.750	8.139
2	1	3.743	10.16	0.912	4.833
	2	3.620	10.30	0.945	2.921
3	1	2.664	9.22	0.963	1.006
	2	2.495	8.99	0.971	0.826
4	1	3.907	14.87	0.836	4.478
	2	4.338	15.33	0.808	3.942
5	1	3.829	12.45	0.939	1.957
	2	3.329	10.90	0.934	3.482
6	1	4.145	15.47	0.956	1.678
	2	3.450	12.77	0.953	1.076
7	1	5.590	13.63	0.746	5.489
	2	5.284	13.15	0.783	4.434
8	1	5.006	15.38	0.717	2.070
	2	5.059	14.55	0.763	2.688
9	1	6.565	17.27	0.726	6.789
	2	6.764	17.66	0.718	6.644
10	1	3.069	10.21	0.903	1.833
	2	3.048	10.54	0.882	2.301
Mean		4.275	13.47	0.851	3.715
STD		1.205	3.08	0.094	2.284

Table 4.2: Test results of the hip joint with mean and standard deviation (STD)

Subject	Trial	RMSE (deg)	NRMSE (%)	R^2	ROM-RMSE (deg)
11	1	3.322	9.90	0.889	3.002
	2	3.106	10.19	0.902	1.837
12	1	2.378	6.79	0.954	2.534
	2	2.567	7.22	0.955	4.727
Mean		2.843	8.52	0.925	3.025
STD		0.444	1.77	0.035	1.232

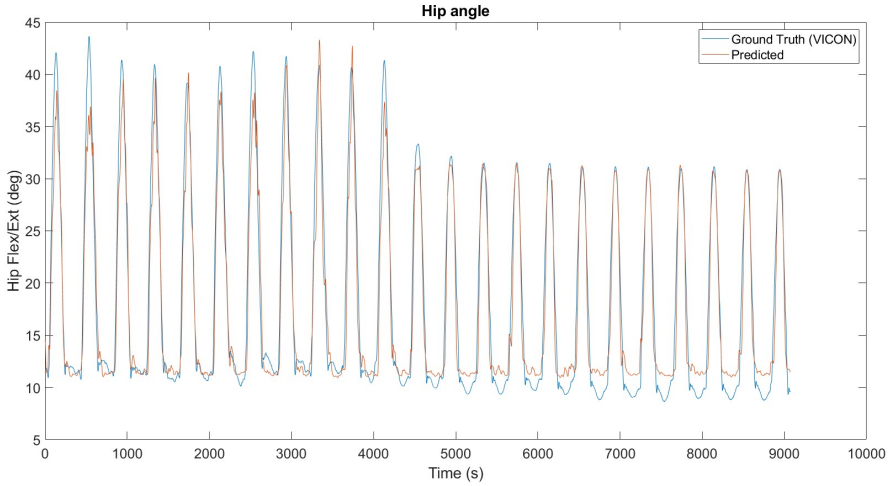

Figure 4.2: Estimated and reference hip angles of subject 11 during trial 1

4.2 Knee Joint

Table 4.3 shows the results of the knee angle predictions for the training data. The average root mean squared value (R^2) for ten participants was greater than 0.85. The RMSE, NRMSE and RMSE-ROM were 6.564°, 12.73 %, and 5.434° respectively.

Table 4.3: Training results of the knee joint with mean and standard deviation (STD)

Subject	Trial	RMSE (deg)	NRMSE (%)	R^2	ROM-RMSE (deg)
1	1	6.282	16.70	0.871	12.253
	2	6.631	19.33	0.911	14.072
2	1	4.590	9.92	0.934	2.321
	2	3.778	7.80	0.947	2.684
3	1	3.174	6.73	0.949	2.492
	2	2.540	5.73	0.963	1.174
4	1	6.436	13.11	0.822	4.460
	2	6.805	13.53	0.800	3.144
5	1	5.381	9.70	0.915	4.867
	2	5.633	10.32	0.913	6.053
6	1	5.888	13.57	0.932	2.177
	2	5.138	11.64	0.936	1.618
7	1	8.513	12.71	0.781	7.613
	2	7.496	10.69	0.822	6.499
8	1	8.455	16.57	0.697	9.394
	2	8.187	15.85	0.744	8.857
9	1	10.300	16.50	0.708	4.662
	2	11.877	18.66	0.693	5.036
10	1	7.454	13.11	0.855	5.676
	2	6.723	12.50	0.837	3.617
Mean		6.564	12.73	0.851	5.434
STD		2.273	3.79	0.090	3.514

The test results for the knee are displayed in table 4.4. In this case, the R^2 was 0.916, the RMSE and NRMSE 4.692º and 8.84% respectively, and the RMSE for the range of motion of 4.597º. Figure 4.3 shows the knee angle's prediction and ground truth, corresponding to subject eleven during the first trial.

Table 4.4: Test results of the knee joint with mean and standard deviation (STD)

Subject	Trial	RMSE (deg)	NRMSE (%)	R^2	ROM-RMSE (deg)
11	1	5.087	9.04	0.887	4.635
	2	4.490	8.83	0.892	2.212
12	1	4.583	8.79	0.940	3.911
	2	4.608	8.69	0.944	7.632
Mean		4.692	8.84	0.916	4.597
STD		0.268	0.15	0.031	2.264

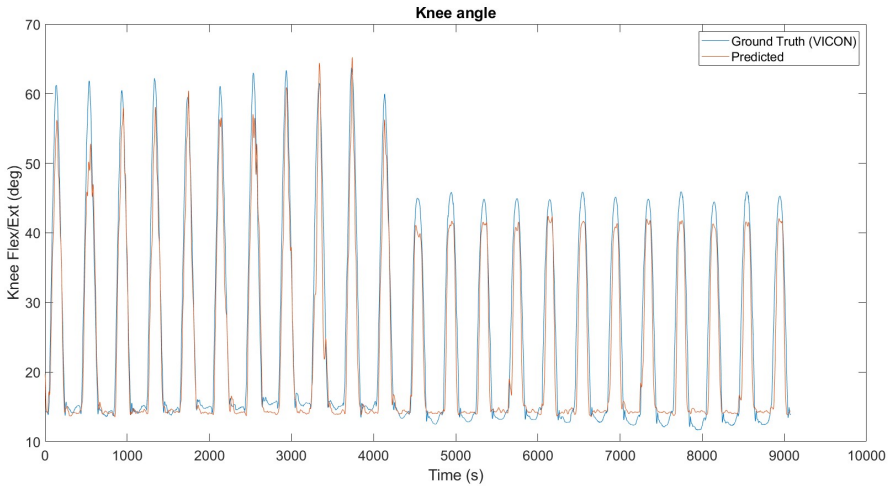

Figure 4.3: Estimated and reference knee angles of subject 11 during trial 1

4.3 Ankle Joint

In table 4.5 the results of the ankle angle predictions for the training data are displayed. The average root mean squared value (R^2) for ten participants was greater than 0.80, while the RMSE and NRMSE were lower than 4.84° and 9.82 %, respectively.

The ROM-RMSE has been divided into dorsiflexion and plantar flexion movements for the ankle results. We obtained a value of 5.542° for dorsiflexion and 7.609° for plantar flexion.

Table 4.5: Training results of the ankle joint with mean and standard deviation (STD)

Subject	Trial	RMSE (deg)	NRMSE (%)	R^2	ROM-RMSE (deg) (Dorsiflexion)	ROM-RMSE (deg) (Plantar flexion)
1	1	3.320	12.45	0.937	3.907	8.121
	2	3.786	8.48	0.843	7.136	8.552
2	1	6.206	9.88	0.741	6.296	1.356
	2	4.500	9.22	0.925	6.282	2.992
3	1	4.369	9.06	0.908	4.930	11.367
	2	3.853	8.62	0.879	5.121	10.114
4	1	4.839	7.00	0.902	9.447	4.894
	2	4.864	8.10	0.892	6.116	6.114
5	1	3.850	10.27	0.752	2.140	3.460
	2	3.946	9.96	0.721	1.211	2.865
6	1	2.915	6.44	0.939	7.507	7.591
	2	2.929	6.29	0.934	8.651	6.670
7	1	6.384	11.85	0.653	5.160	8.870
	2	6.609	11.19	0.613	5.159	9.693
8	1	4.536	9.10	0.804	6.894	4.101
	2	6.763	15.11	0.532	9.405	16.853
9	1	8.248	11.85	0.892	7.107	16.103
	2	9.417	13.91	0.818	4.198	16.758
10	1	2.987	8.97	0.727	2.111	3.717
	2	2.322	8.73	0.761	2.067	1.979
Mean		4.832	9.82	0.809	5.542	7.609
STD		1.883	2.33	0.118	2.422	4.805

The outcome performance for the ankle angle among subjects eleven and twelve, which are the test results, are displayed in table 4.6. In this case, the R^2 was 0.798, the RMSE and NRMSE 3.706º and8.38% respectively. Concerning the range of motion, the RMSEs obtained were 9.997º for dorsiflexion and 4.490º for plantar flexion. Figure 4.4 shows the prediction and the reference angles of the ankle joint, corresponding to subject eleven during the first trial.

Table 4.6: Test results of the ankle joint with mean and standard deviation (STD)

Subject	Trial	RMSE (deg)	NRMSE (%)	R^2	ROM-RMSE (deg) (Dorsiflexion)	ROM-RMSE (deg) (Plantar flexion)
11	1	4.863	9.27	0.791	11.030	8.042
	2	4.078	8.36	0.779	10.954	4.114
12	1	2.650	6.49	0.835	9.084	1.540
	2	3.231	9.40	0.787	8.922	4.266
Mean		3.706	8.38	0.798	9.997	4.490
STD		0.969	1.34	0.025	1.151	2.678

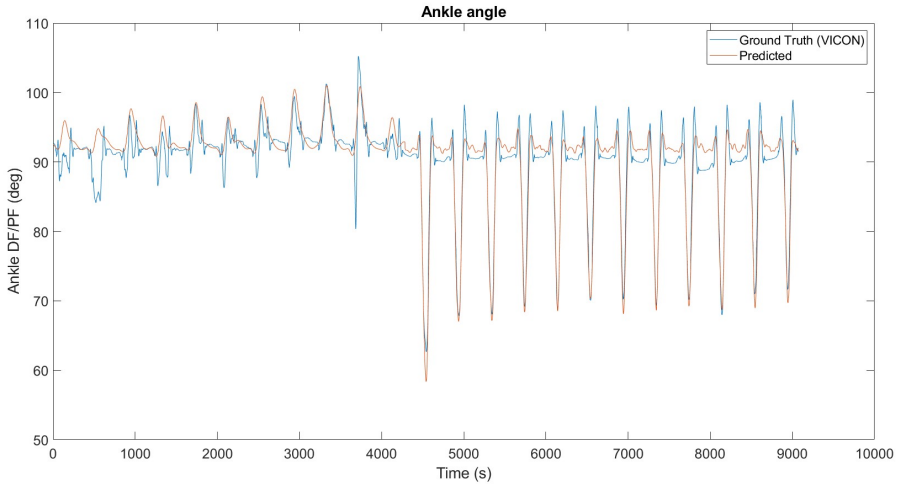

Figure 4.4: Estimated and reference ankle angles of subject 11 during trial 1

5 Discussion

In the test subjects scenario, a R^2 of 0.925 for the hip angle was obtained. These are surprisingly good results. A ROM-RMSE of 3.025º is good enough to track patient data over rehabilitation procedures quantitatively. Although we have access to this data directly from the VEMOTION device, it is interesting to consider other methods to track it. The current method can be used to verify the estimated hip angle by the VEMOTION.

Concerning the knee angles, we observe a significantly higher NRMSE ($\approx 18\%$) in the prediction for subject one. Due to their biomechanical structure, this subject performed shallower movements, having the slightest difference between maximum and minimum values of the tested subjects. A range of 39.47º compared to the mean of 48.08º.

In spite of presenting similar behaviours during the motion, the results for the hip angle estimation are generally better than the knee. Specially with respect to the NRMSE. This can be caused because the range of motion of the hip is typically wider than the knee, so the relative error is smaller.

Regarding the ankle angle, the error of the range of motion estimation during dorsiflexion movement was larger than the plantar flexion, with an NRMSE of 9.99 % and 4.49 % for the test results, respectively. We hypothesize that this could be caused because the angle variation during the plantar flexion movement is more profound, therefore capturing a stronger signal in the accelerometer that results in a more meaningful input for the network and, consequently, a better prediction.

Further, we observed that the ankle joint has the most variable inter-participant results. We assume that the height, positioning, and length of the subject's lower limbs directly affect the values.

For the three joint angles, it is a generalized occurrence that, contrary to what was expected, the test results are better than the training ones. The train/test split percentage most likely causes this. Due to the limited number of subjects, it was impossible to implement a more balanced data set for training and testing with extensive enough training data. Also, cross-validation, due to computational costs, was not feasible.

In general, standard deviations are substantially more minor than average values. This indicates that this approach performs consistently across all test individuals and is robust to inter-participant differences.

The fact that the model was trained only with the right leg data has to be considered. Results of left lower limb kinematics still need to be addressed, being a possible solution to create a different model for the left side in case the current one does not work. Nonetheless, as the input is a 400 ms window, the evaluated side (left or right) should not affect the performance. Since left and right leg movements are frequently unequal, especially in people with disabilities, this

problem must be addressed in the future.

All the trials were captured with a verticalization angle of 50°. No variability was introduced regarding this parameter, so the method's robustness concerning this subject is unknown. Nevertheless, due to the positioning of the accelerometers, their system of reference would also change with the verticalization angle. Therefore, this parameter's variations should not affect the model's performance in any way.

Also, the different pattern movements of the ankle (dorsi and plantar flexion) were clearly differentiated during the trials. In clinical application, the patients normally do not focus on a specific pattern, therefore a test with no pattern instructions with a healthy subject should be done to verify the network.

The present thesis is inspired by the Gholami et al. [13] research. In this study, the results in the inter-participant scenario, the error of the ankle joint angle estimation was significant, with an NRMSE of 11% and an R^2 of 0.78. This may be caused because gait analysis has more degrees of freedom, and the movement is less restricted. They also used only one accelerometer, whereas we employed two of them.

Although the NRMSE values for the predictions might seem high, this project aimed to develop an accessible, relatively cheap, and non-invasive method of collecting patient data in ICUs. So the results obtained are helpful to get a general insight into the behavior of the lower limb joint angles during VEMOTION rehabilitation. Principally being able to differentiate between dorsiflexion and plantar flexion movements.

6 Conclusion

In this project, we investigated the performance of hip, knee, and ankle estimation on the sagittal plane during VEMOTION rehabilitation procedure. The Gholami et al. [13] approach to gait analysis was implemented in our particular case. A convolutional neural network was used to estimate the joint angles.

The prediction was made using raw data from accelerometers positioned on the VEMOTION device as input for the network. Hence, this project aimed at obtaining an easy, non-invasive method of collecting patient data in ICUs.

Twelve subjects were tested in two different trials, performing plantar flexion and dorsiflexion movements in every one of them. The network was trained with the ten first subjects and tested on the remaining two. The ground truth data for verification was captured using the Vicon System, the gold standard for human motion capture procedures.

Although the accuracy of the results could be better, this system has proven to help get a general insight into the behavior of the lower limb joint angles during VEMOTION rehabilitation. Especially being able to differentiate between dorsiflexion and plantar flexion movements. Consequently, we can now quantitatively assess the performance changes in chronic stroke patients, where limited ankle range of motion is a common issue.

The initial idea was to design only one network for which the output consists of simultaneously predicting the three joint angles. Nevertheless, we realized that the performance was better with a slightly different preprocessing for the ankle joint, thus splitting the system into three different networks.

Further steps of this work could be including surface electromyography data for the ankle movement and comparing how it changes during the different joint motion patterns. Using this approach could tackle the inability to lift the foot during the swing phase of gait, a common problem among post-stroke patients known as foot drop [29].

It could also be interesting to compare the performance of other deep learning models, like feedforward neural network (FNN) [4], or Feedback Process Neural Networks [6] instead of the convolutional approach employed.

Another possibility would be to implement a multi-input model, where extra parameters, like the subject's height, are incorporated into the network. Height plays an essential role in the patient's position on the bed, hence being a key factor for the maximum and minimum values of the angles during the motion.

For better results, although being a more complex and expensive method due to the number of sensors required, a model-based approximation to the problem would be another solution. In this case, kinematic constraints of the human body are implemented to IMU's collected data, recreating the kinematic model from there [8].

7 References

[1] Abayneh Alamer et al. “Effect of Ankle Joint Mobilization with Movement on Range of Motion, Balance and Gait Function in Chronic Stroke Survivors: Systematic Review of Randomized Controlled Trials”. In: *Degenerative Neurological and Neuromuscular Disease* 11 (2021), p. 51.

[2] Kai-Nan An. “Kinematic analysis of human movement”. In: *Annals of biomedical engineering* 12.6 (1984), pp. 585–597.

[3] RJ Baker et al. “The conventional gait model-success and limitations”. In: *Handbook of human motion* (2018), pp. 489–508.

[4] George Bebis and Michael Georgiopoulos. “Feed-forward neural networks”. In: *IEEE Potentials* 13.4 (1994), pp. 27–31.

[5] Matteo Bigoni et al. “Does kinematics add meaningful information to clinical assessment in post-stroke upper limb rehabilitation? A case report”. In: *Journal of physical therapy science* 28.8 (2016), pp. 2408–2413.

[6] Chunshui Cao et al. “Look and think twice: Capturing top-down visual attention with feedback convolutional neural networks”. In: *Proceedings of the IEEE international conference on computer vision*. 2015, pp. 2956–2964.

[7] Iñaki Díaz, Jorge Juan Gil, and Emilio Sánchez. “Lower-limb robotic rehabilitation: literature review and challenges”. In: *Journal of Robotics* 2011 (2011).

[8] Eva Dorschky et al. “Estimation of gait kinematics and kinetics from inertial sensor data using optimal control of musculoskeletal models”. In: *Journal of biomechanics* 95 (2019), p. 109278.

[9] Alexander Duschau-Wicke, Andrea Caprez, and Robert Riener. “Patient-cooperative control increases active participation of individuals with SCI during robot-aided gait training”. In: *Journal of neuroengineering and rehabilitation* 7.1 (2010), pp. 1–13.

[10] A Findlow et al. “Predicting lower limb joint kinematics using wearable motion sensors”. In: *Gait & posture* 28.1 (2008), pp. 120–126.

[11] Jing Gao et al. “A Parametric Identification Method of Human Gait Differences and its Application in Rehabilitation”. In: *Applied Sciences* 9.21 (2019), p. 4581.

[12] Gert Jan Gelderblom et al. “Rehabilitation robotics in robotics for healthcare; a roadmap study for the European Commission”. In: *2009 IEEE international conference on rehabilitation robotics*. IEEE. 2009, pp. 834–838.

[13] Mohsen Gholami, Christopher Napier, and Carlo Menon. “Estimating lower extremity running gait kinematics with a single accelerometer: a deep learning approach”. In: *Sensors* 20.10 (2020), p. 2939.

[14] Mohsen Gholami et al. “Lower body kinematics monitoring in running using fabric-based wearable sensors and deep convolutional neural networks”. In: *Sensors* 19.23 (2019), p. 5325.

[15] M Girone et al. “A Stewart platform-based system for ankle telerehabilitation”. In: *Autonomous robots* 10.2 (2001), pp. 203–212.

[16] Mohammed M Hamdi et al. “Lower limb motion tracking using IMU sensor network”. In: *2014 Cairo International Biomedical Engineering Conference (CIBEC)*. IEEE. 2014, pp. 28–33.

[17] Stefan Hesse et al. “Upper and lower extremity robotic devices for rehabilitation and for studying motor control”. In: *Current opinion in neurology* 16.6 (2003), pp. 705–710.

[18] Lihua Huang, Ryan Ryan Steger, and H Kazerooni. "Hybrid control of the Berkeley lower extremity exoskeleton (BLEEX)". In: *ASME International Mechanical Engineering Congress and Exposition*. Vol. 42169. 2005, pp. 1429–1436.

[19] Walter Johnson et al. "Stroke: a global response is needed". In: *Bulletin of the World Health Organization* 94.9 (2016), p. 634.

[20] Bhaben Kalita, Jyotindra Narayan, and Santosha Kumar Dwivedy. "Development of active lower limb robotic-based orthosis and exoskeleton devices: a systematic review". In: *International Journal of Social Robotics* 13.4 (2021), pp. 775–793.

[21] Serkan Kiranyaz et al. "1D convolutional neural networks and applications: A survey". In: *Mechanical systems and signal processing* 151 (2021), p. 107398.

[22] Bart HW Koning et al. "Driving a musculoskeletal model with inertial and magnetic measurement units". In: *Computer methods in biomechanics and biomedical engineering* 18.9 (2015), pp. 1003–1013.

[23] HI Krebs, and BT Volpe. "Rehabilitation robotics". In: *Handbook of clinical neurology* 110 (2013), pp. 283–294.

[24] Yann LeCun, Yoshua Bengio, and Geoffrey Hinton. "Deep learning". In: *nature* 521.7553 (2015), pp. 436–444.

[25] Dariush Mozaffarian et al. "Heart disease and stroke statistics—2015 update: a report from the American Heart Association". In: *Circulation* 131.4 (2015), e29–e322.

[26] Gergely Nagymáté and Rita M Kiss. "Application of OptiTrack motion capture systems in human movement analysis: A systematic literature review". In: *Recent Innovations in Mechatronics* 5.1. (2018), pp. 1–9.

[27] Pedro Nogueira. "Motion capture fundamentals". In: *DOCTORAL SYMPOSIUM IN INFORMATICS ENGINEERING*. 2011, p. 303.

[28] Pietro Picerno. "25 years of lower limb joint kinematics by using inertial and magnetic sensors: A review of methodological approaches". In: *Gait & posture* 51 (2017), pp. 239–246.

[29] Rakesh Pilkar, Mathew Yarossi, and Karen J Nolan. "EMG of the tibialis anterior demonstrates a training effect after utilization of a foot drop stimulator". In: *NeuroRehabilitation* 35.2 (2014), pp. 299–305.

[30] Henning Schmidt et al. "Gait rehabilitation machines based on programmable footplates". In: *Journal of neuroengineering and rehabilitation* 4.1 (2007), pp. 1–7.

[31] Michael Schünke et al. *Lernatlas der Anatomie*. 2018.

[32] Thomas Seel, Jorg Raisch, and Thomas Schauer. "IMU-based joint angle measurement for gait analysis". In: *Sensors* 14.4 (2014), pp. 6891–6909.

[33] Erfan Shahriari et al. "Energy-based Adaptive Control and Learning for Patient-Aware Rehabilitation". In: *IEEE International Conference on Intelligent Robots and Systems* (2019), pp. 5671–5678. ISSN: 21530866. DOI: 10.1109/IROS40897.2019.8968249.

[34] Geert Sulter, Christel Steen, and Jacques De Keyser. "Use of the Barthel index and modified Rankin scale in acute stroke trials". In: *Stroke* 30.8 (1999), pp. 1538–1541.

[35] Vicon Motion Systems. *What is Motion Capture? Vicon About us*. 2022. URL: https://www.vicon.com/about-us/what-is-motion-capture/ (visited on 03/25/2022).

[36] Anthony A. Vandervoort. "Ankle mobility and postural stability". In: *Physiotherapy Theory and Practice* 15 (2 1999), pp. 91–103. ISSN: 09593985. DOI: 10.1080/095939899307793.

[37] Jan F Veneman et al. "Design and evaluation of the LOPES exoskeleton robot for interactive gait rehabilitation". In: *IEEE Transactions on neural systems and rehabilitation engineering* 15.3 (2007), pp. 379–386.

[38] Derick T Wade et al. "Physiotherapy intervention late after stroke and mobility." In: *British Medical Journal* 304.6827 (1992), pp. 609–613.

[39] Frank J Wouda et al. “Estimation of vertical ground reaction forces and sagittal knee kinematics during running using three inertial sensors”. In: *Frontiers in physiology* 9 (2018), p. 218.

[40] Jia-fan Zhang et al. “5-Link model based gait trajectory adaption control strategies of the gait rehabilitation exoskeleton for post-stroke patients”. In: *Mechatronics* 20.3 (2010), pp. 368–376.

[41] Xue Zhang, Zan Yue, and Jing Wang. “Robotics in lower-limb rehabilitation after stroke”. In: *Behavioural neurology* 2017 (2017).